Indian Journal of Pure & Applied Physics
Vol. 60, December 2022, pp. 982-988
DOI: 10.56042/ijpap.v60i12.66425

Conduction Mechanism and Dielectric Properties in Polyaniline/Titanium Dioxide Composites

Asha[a*], Sneh Lata Goyal[b], Rachna Dhankhar[c], Rahul Sharma[d] & Arvind Sharma[e]

[a]Department of Basic and Applied Sciences, Bhagat Phool Singh Mahilla Vishwavidyalaya, Khanpur Kalan, Sonipat, Haryana- 131 305, India

[b]Department of Physics, Guru Jambheshwar University of Science and Technology, Hisar, Haryana- 125 011, India

[c]Department of Chemistry, Maharshi Dayanand University, Rohtak, Haryana- 124 001, India

[d]CSIR- National Physical Laboratory, New Delhi-110 012, India

[e]Department of Basic and Applied Science, National Institute of Technology, Arunachal Pradesh, Jote, 791 113, India

Received 11 September 2022; accepted 21 November 2022

The conductivity and dielectric properties of polyaniline (PANI) and PANI/TiO_2 composites have been studied over a temperature range (313-393 K) and frequency range (25 Hz- 50 MHz). The nature of temperature and frequency-dependent conductivity can be explained by Jonscher's universal power law and used to find the related parameters such as frequency exponent (s), dc conductivity (σ_{dc}), and crossover frequency (ω_H). Besides, the frequency exponent analysis through a distinct model suggests that the conduction occurred through small polaron tunnelling in all compositions and at different temperatures. On the other hand, the enthalpy of migration (H_m), dissociation enthalpy of cation from its indigenous location alongside a compensating center (H_f), and the activation energy were also calculated using the Arrhenius relation. The temperature-dependent dc conductivity was examined in the framework of the theoretical model; Mott's variable range hopping model (VRH) and experimental results were in good agreement with the 3-dimensional VRH model. As a function of temperature, dielectric constants (ε' and ε") increase while decreasing with an increasing dopant. Being such a high dielectric constant value, these composites can be used as frequency converters, modulators, and dielectric amplifiers.

Keywords: Polyaniline; Conductivity; Activation energy; Dielectric constants

1 Introduction

The conducting polymers have turned out to be marathon materials in diverse areas such as EMI shielding, energy storage, and environmental remediation, and their exclusive optoelectronic, chemical, and thermal properties. The conductivity of the indicated materials could be diversified from semiconducting to the metallic range by doing proper doping, which provides a novel notion for the transport of charge. Due to this property, conducting polymers are useful for several technological purposes, for instance, active electrode materials in energy storage[1], optoelectronic devices[2,3], display devices[4,5], corrosion inhibitors[6,7] and sensors[8-11]. Conducting polymers in general and Polyaniline (PANI) is the most attractive conducting polymer as it can be easily synthesized in an aqueous medium, has good environmental stability, and has extraordinary electrical properties. Research in the field of such polymers is effective when some suitable modifications are done to these polymers to improve their applicability. Some of these modifications can be done by doping with transition metal oxides such as SnO_2[12], CeO_2[13], V_2O_5[14], TiO_2[15], ZnO[16], Fe_3O_4[17], ZrO_2[18], Y_2O_3[19], CuO[20], CrO_3[21,] etc. coalesce in some unique manner with the conducting polymers to produce their composites. Various properties of PANI, especially conductivity, vary significantly in doped form leading to exciting applications.

TiO_2 (titanium dioxide) is non-hazardous material having high thermal and chemical stability. It is an essential semiconductor that exhibits thermally and environmentally stable dielectric properties and is characterized by a relatively high dielectric constant utilized in the microwave TiO_2 absorber. TiO_2 nanoparticles have been proclaimed by several researchers intended for various applications[15,22]. In composite form with PANI, it has potential applications in charge storage, photovoltaic cells, anticorrosion coating, photocatalysis, *etc*.

The PANI and PANI loaded with TiO_2 composite (by changing the percentage weight of the titanium

*Corresponding author:
(E-mail: arana5752@gmail.com)

dioxide in polyaniline) have been prepared in the current research. Moreover, the study of the dielectric properties of PANI loaded with TiO_2 composites and the AC conductivity has been reported.

2 Experimental Details

2.1 Synthesis of PANI

In a typical synthesis process, PANI has been prepared via chemical oxidation of 0.2 M aniline (Aldrich) using 0.25 M ammonium peroxidisulphate as an oxidizing agent (Aldrich). Before oxidation, both solutions were cooled within the temperature range of 0-4 ^oC and mixed dropwise on an ice bath. The reaction mixture was stirred for 2h and left overnight for completion of the polymerization process in the refrigerator. The as obtained PANI was washed several times with 1M HCl solution to remove the unreacted phases, followed by final washing with acetone. The as obtained PANI material (emeraldine) was dried at 45 ^oC under vacuum[16].

2.2 Preparation of PANI/TiO_2 composites

The various PANI loaded titanium dioxide (TiO_2) composites were synthesized by addition of 20, 40, and 50 percentage by weight of the titanium dioxide (Aldrich) to the solution of 0.2 M aniline hydrochloride that had been dissolved in distilled water prior to the oxidation process for 2 h so that the powder of titanium dioxide remains suspended within the solution. Using the process same as a synthesis of PANI, PANI loaded with TiO_2 composites were synthesized and termed t20, t40, and t50, sequentially regulated by the amount (percentage by weight) of addition of TiO_2.

2.3 Analytical techniques

The impedance spectroscopy of the samples (pellets of 1.2 cm diameter and polished with silver paint) has been carried out on a Hioki IM3570 Impedance Analyzer in a frequency range of 25Hz-5MHz and temperature range of 293K-393K. Different parameters (dielectric loss, electrical modulus, *etc*.) have been calculated from the data obtained from impedance spectroscopy.

3 Results and discussion

The entire frequency-dependent conductivity σ′ (ω) remains constant for PANI loaded with TiO_2 composites along with PANI till a definite frequency after that, it flaunts a dispersive behavior, *i.e*., σ′ (ω) rises by the rise in frequency that is a characteristic behavior for the disorder materials. Various researchers as well detected the same kind of behaviour[23-25]. A distinctive deviation of σ′ (ω) with the frequency at 353K for PANI plus PANI loaded with TiO_2 composites has been represented in Fig. 1. A similar variation for PANI/TiO_2 composite (t20) at different temperatures is also presented in Fig. 2.

Persual of the data represented in Fig. 2, it has been observed that the conductivity also increases with the

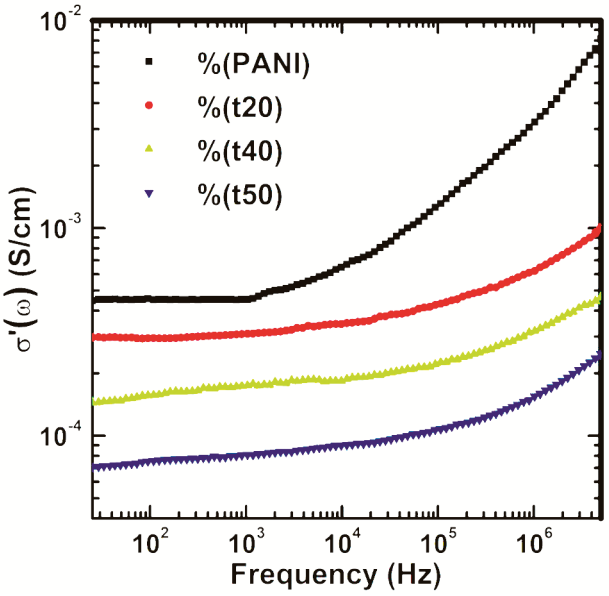

Fig. 1 — Variation of the conductivity with the frequency for PANI and PANI/TiO_2 composites at 353K.

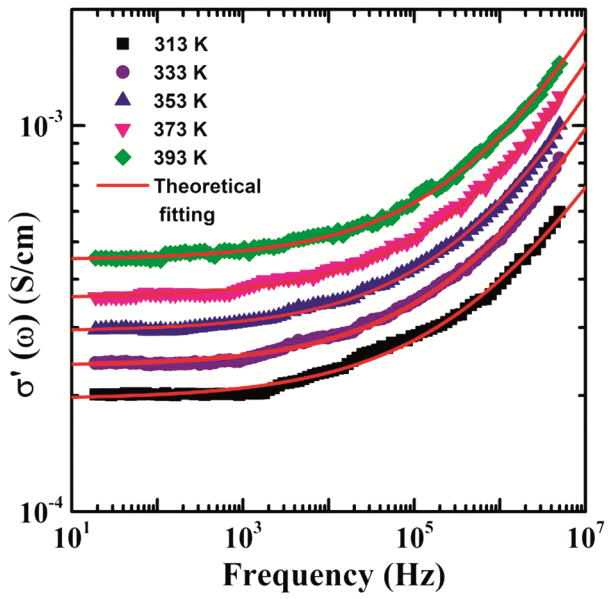

Fig. 2 — Variation of conductivity with frequency for PANI/TiO_2 composite (t20) at different temperatures.

increase in temperature. This enhancement in the conductivity with the rising temperature may be because of the increment in the free charge carriers with the increment in the temperature[26,27]. The conductivity varies inversely with the concentration of TiO_2 in PANI.

Jonscher's power law determines the semiconductor's total conductivity (σ' (ω)) as:

$$\sigma'(\omega) = \sigma_{dc}\left[1+\left(\frac{\omega}{\omega_H}\right)^s\right] \quad \ldots(1)$$

where σ_{dc}: frequency independent dc conductivity, ω_H: crossover frequency untying the dc plateau region from the dispersive conduction; s: frequency exponent whose value lies between 0 to 1[28-30].

The value of ω_H, $\sigma_{dc,}$ and s has been obtained by situating experimentally obtained σ' (ω) data at various temperatures in equation (1), *i.e.*, Jonscher's universal power law. The Jonscher's power law perfectly fits experimental data for PANI/TiO_2 composites, as shown in Fig. 2, indicating that Jonscher's power law holds for the composites, and such results are already observed by some other researchers also[27,29]. The values of dc conductivity (σ_{dc}) have also been determined by calculating resistance from ohm's law already published elsewhere[31]. On comparing the values of dc conductivity from both methods, it was observed that the dc conductivity values obtained from the conventional ohm's law method are always less than that obtained from impedance spectroscopy. The low conductivity in ohm's law may be due to the accumulation of charge carriers opposing the current flow.

The values of s calculated by fitting Jonscher's power law lie between 0.35 and 0.65, as shown in Fig. 3. The conduction mechanism may be determined from the variation of the frequency exponent. Various conventional models, such as Correlated barrier hopping (CBH)[32], small polaron tunneling[33], electron tunnelling, and large polaron tunnelling, *etc*., have been postulated to access the conduction mechanism[34-36].

Persual of the data presented in Fig. 3 shows that the value of s for PANI and PANI loaded with TiO_2 composites varies directly with temperature. And this is the quality of small polaron tunnelling, and such behavior could be described by the small polaron tunnelling model given by

$$s = 1 - \frac{4}{\ln\left(\frac{1}{\omega\tau_0}\right) - \frac{W_H}{kT}} \quad \ldots(2)$$

Where k is the Boltzmann constant, W_H is the barrier height for an infinite site separation, T is temperature, ω is the angular frequency, and τ_0 is the relaxation time [33,37].

If the conduction is due to a defect mechanism, then

$$n = N\exp\left(-\frac{G_f}{kT}\right) = N\exp\left(\frac{S_f}{k}\right)\times\ exp\left(-\frac{H_f}{kT}\right) \quad \ldots(3)$$

where n is the number of mobile charge carriers, N is the total number of charge carriers, S_f is entropy, and G_f and H_f are the free energy for dissociating the cation from its original site to the compensating center and enthalpy, respectively.

Crossover frequency (ω_H) is given by

$$\omega_H = \omega_0\exp\left(\frac{S_m}{k}\right)\times\exp\left(-\frac{H_m}{kT}\right) \quad \ldots(4)$$

and dc electric conductivity is given by

$$\sigma_{dc} = \frac{NZ^2e^2d^2\Upsilon\omega_0}{kT}\exp\left(\frac{S_f+S_m}{k}\right)\times\exp\left(-\frac{H_f+H_m}{kT}\right) \quad \ldots(5)$$

Where ω_0 is attempt frequency, d is the jump distance, γ is a constant consisting of geometric plus correlation factors, and H_m and $S_m$are enthalpy and entropy of migration, respectively.

Calculation of slopes of plots ln (σ_{dc}T) versus 1/T and ln (ω_H) versus 1/T determine the value of

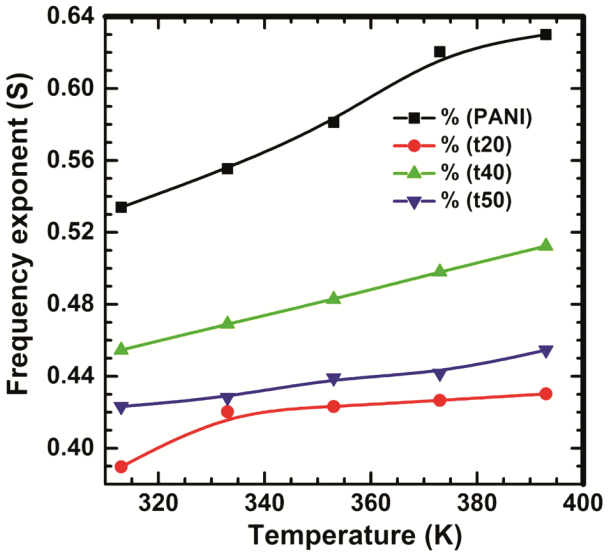

Fig. 3 — Frequency exponent (S) variation with the temperature for PANI and PANI/TiO_2 composites.

($H_f + H_m$) and H_m, respectively, using equations (4) and (5), and the calculated values are presented in Table 1. The slopes are computed using linear fitting (Figs. 4 and 5). The data in Table 1 shows that the $H_f > 0$ for the entire sample indicates that the mobile charge carriers are less than the total number of charge carriers.[38]

Data of electrical conductivity for all the samples comply with the Arrhenius relation[39] given by:

$$\sigma_{dc} = \sigma_0 \exp\left(-\frac{W}{kT}\right) \quad \ldots (6)$$

W is the carrier activation energy, k is the Boltzmann constant, and σ_0 is the pre-exponential factor.

It is clear from equation (6) that the activation energy can be calculated from the slope of the curve ln σ_{dc} versus 1/T. The slope is calculated by linear fitting (as shown in Fig. 6) and represented in Table 1 for all the samples. It is observed from Table 1 the value of activation energy is found to increase with an increase in the concentration of TiO_2, which implies the decrease in conductivity with increasing content of TiO_2.

Table 1 — Migration Enthalpy (H_m), enthalpy of the cation from its original site next to a compensating center (H_f), and Activation Energy (W) in eV for PANI and PANI/TiO_2 composites

Parameter	PANI	t20	t40	t50
$H_f + H_m$	0.129	0.140	0.155	0.131
H_m	0.040	0.027	0.034	0.068
H_f	0.089	0.113	0.121	0.063
W	0.099	0.110	0.117	0.127

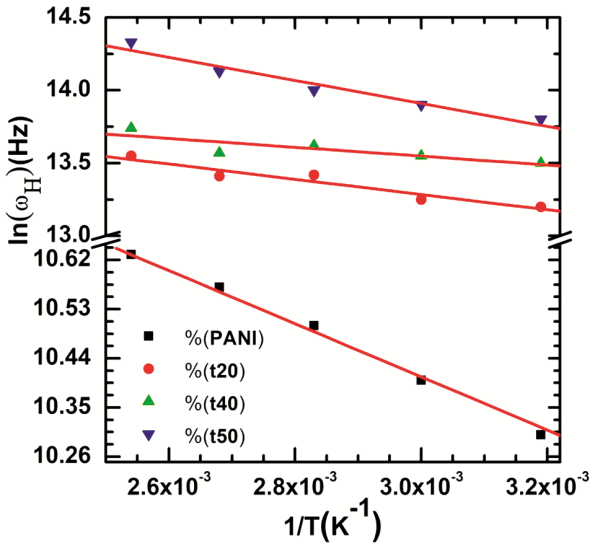

Fig. 4 — Linear plot of ln (ω_H) versus 1/T for PANI and PANI/TiO_2 composites.

The dependence of the dc conductivity σ_{dc} of disarranged semiconducting materials on the temperature (T) can be explained with the help of Mott's variable range hopping (VRH) model, which is a possible mechanism for charge transport in the conducting polymers at low temperatures. Mott's model for hopping is given by

$$\sigma_{dc} = \sigma_0 e^{-\left(\frac{T_0}{T}\right)^{\gamma}} \quad \ldots (7)$$

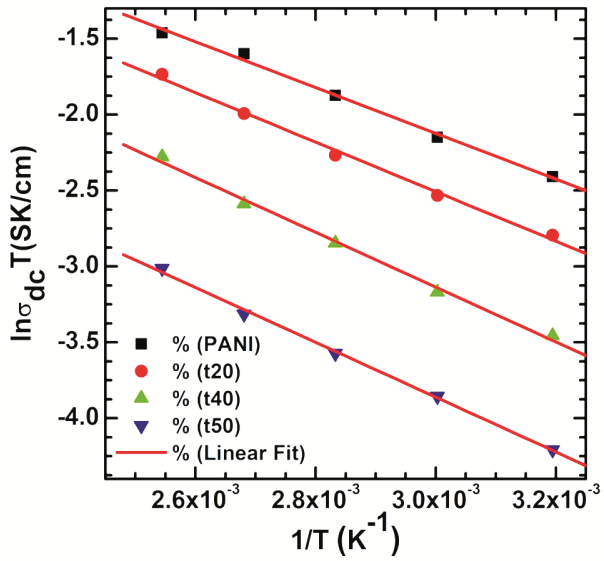

Fig. 5 — Linear Fit of ln (σ_{dc}T) versus 1/T for PANI and PANI/TiO_2 composites.

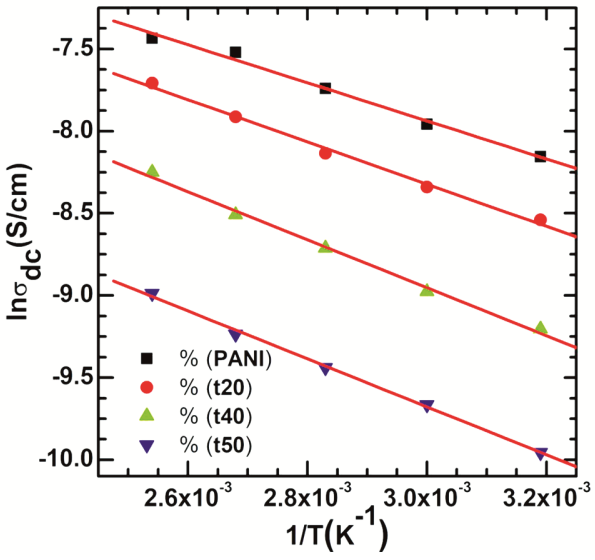

Fig. 6 — Linear plot of ln σ_{dc} versus 1/T of PANI and PANI/TiO_2 composites.

where T_0 is Mott's characteristic temperature related to the extent of localization of electronic wave function, and σ_0 is a higher temperature limit for conductivity. Conducting medium dimensionality could be found by the exponent $\gamma = 1/(1+d)$. Probable values of γ for three, one, and two-dimensional systems are 1/4, 1/2, and 1/3, correspondingly [40]. But in the present case, it is observed that the plot of ln $\sigma_{dc}(T)$ vs. $T^{(-1/4)}$ gives better linear fitting (~ 0.999) in comparison to the respective Arrhenius plot, *i.e.*, ln $\sigma_{dc}(T)$ versus 1/T (~ 0.99) of the experimental data. Thus, the three-dimensional (3D) charge transports occur in all the samples, even at high temperatures.

Both the real the imaginary parts of the dielectric constant are as certained. The real part of the frequency-dependent dielectric constant (ε') at 353K is presented in Fig. 8, and Fig. 9 shows its change with frequency for PANI/TiO_2 composite (t20) at different temperatures. Analyzing the presented statistics in Fig. 8 demonstrates that in the case of PANI/titanium dioxide composites, the real part of the dielectric constant decreases in a frequency range of 10^4 Hz and becomes constant for an additional increase in the frequency. This resembles the behaviour of disarranged material. The reason could be that the ions are attached firmly to the polymer chain and cannot combat the field effect with increased frequency[41].

Also, it is clear from Fig. 9 that the dielectric constant ε' increases with increasing temperature. The increase in the real part with increasing temperature shows that polarization ratio varies directly with temperature, and dielectric dispersion depends on temperature[42].

The value of ε' at 100 Hz is 7.023×10^5 to 2.37×10^6 for PANI and varies from 1.31×10^5 to 1.3×10^6 for PANI/TiO_2 composites. Such a significant value of the real part of the dielectric constant (permittivity) is usual, although a few researchers also stated values of ε' in the range mentioned above[25].

Figure 10 represents the change in the imaginary dielectric constant (ε") by the change in frequency for pure PANI and PANI loaded with TiO_2 at 333K.

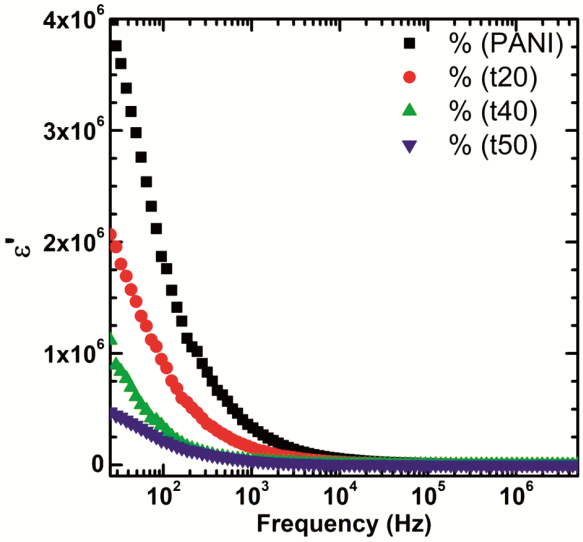

Fig. 8 — ε' variation as a frequency function for TiO_2 loaded with PANI and PANI at 353K.

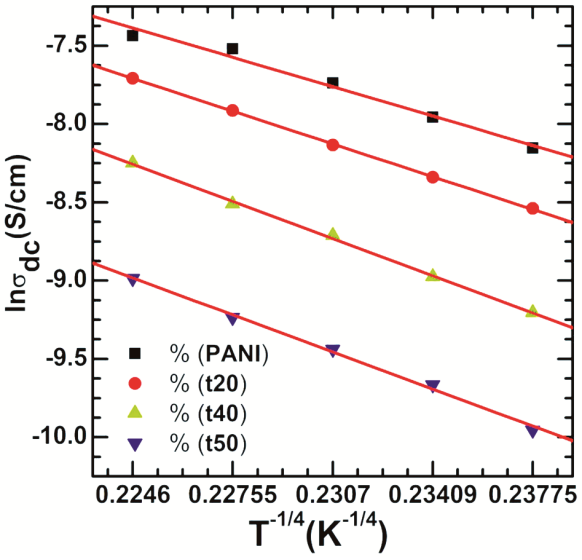

Fig. 7 — Variation of ln(σ_{dc}) with $T^{-1/4}$ of pure PANI and PANI loaded with TiO_2 composites.

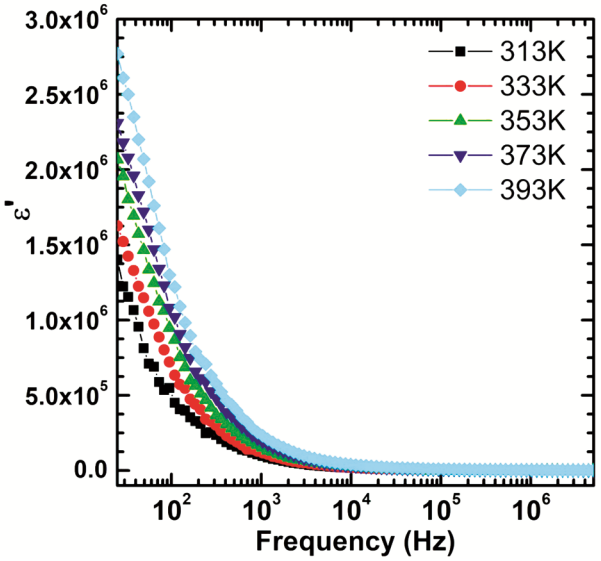

Fig. 9 — ε' variation for TiO_2 loaded with PANI (for t20) as a frequency function at different temperature.

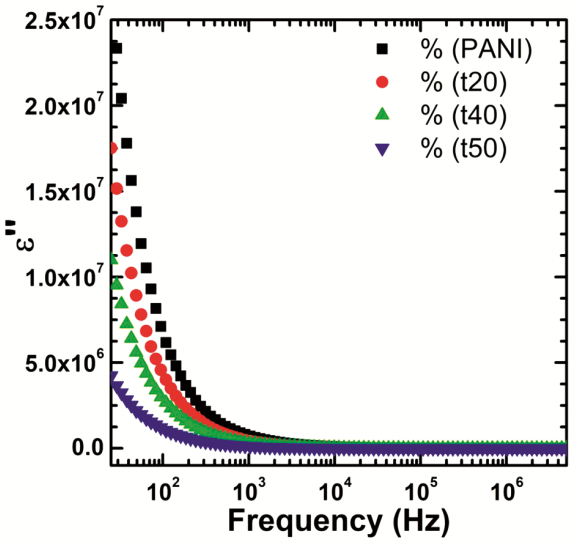

Fig. 10 —Variability of ε" as a frequency function for TiO_2 loaded with PANI and PANI at 333K.

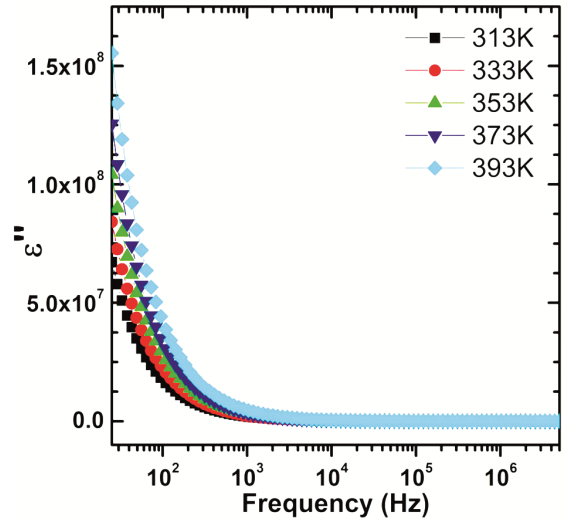

Fig. 11 — Variability of ε" for PANI/TiO_2 composite (t40) as a frequency function at various temperature.

It drops off approximately linearly for a pure PANI along with all its composites at a lower frequency and then shows a constant small value plateau at a higher frequency. This behaviour indicates that these materials are lossless materials at higher frequencies[43].

The imaginary part of the dielectric constant varies inversely with the concentration of TiO_2. The deviation of ε" with the frequency at different temperatures for PANI/TiO_2 composite (t40) is shown in Fig. 11. The Figure demonstrates that the value of ε" varies directly with temperature. The entire ε" outcome follows the conductivity manner. The experimental variation in conductivity is accountable for variation in the dielectric constant behavior of the composites.

4 Conclusions

The ac and dc conductivity of titanium dioxide doped PANI had been examined in the frequency range of 25 Hz-50 MHz plus the temperature range of 313-393 K. The conductivity increases with the increasing temperature but decreases with increasing concentration. The total and dc conductivity for all the compositions agreed with Jonscher's power law and Mott's variable range hopping model. A variety of factors such as frequency exponent (s), dc conductivity (σ_{dc}), and crossover frequency (ω_H) have been determined with the help of conjectural situating of the experimental data using Jonscher's power law. The observation is that with the TiO_2 addition in PANI, the amount of mobile charge carriers decreases, which justifies the reduction in conductivity value. Also, the small polaron tunnelling model describes the conduction mechanism of the virgin sample and all the composites. Variation of dielectric constant with frequency for PANI and all its composites was also studied at varying temperatures. The imaginary and real parts of the constant dielectric increase with increasing temperature and decrease with increasing doping concentration. Also, the value of a dielectric constant is very high. Being such a high dielectric constant value, these composites can be used as frequency converters, modulators, and dielectric amplifiers.

Conflict of Interest

The authors declare that they have no conflicts of interest.

References

1 Nakajima T & Kawogoc T, *Synth Met*, 28 (1989) 544.
2 Kumar G, Shivashanmugam A, Muniyandi N, Dhawan S K & Trivedi D C, *Synth Met,* 50 (1996) 279.
3 Chano S & Wrington M S, *J Am Chem Soc,* 109 (1996) 6627.
4 Kelly F M , Meunier L, Cochrane C & Koncar V, *Displays*, 34 (2013) 1.
5 Dhawan S K & Trivedi D C, *J Appl Electrochem,* 22 (1992) 565.
6 Sathiyanarayanan S, Dhawan S K, Trivedi D C & Balakrishanan K, *Corros Sci,* 33 (1992) 1831.
7 Sathiyanarayanan S, Balakrishanan K, Dhawan S K & Trivedi D C, *Electrochim Acta,* 39 (1994) 831.
8 Arafa I M, El-Ghanem H M & Bani-Doumi K A, *J Inorg Organomet Polym,* 23 (2013) 365.

9 Ayad M M, Salahuddin N A, Minisy I M & Amer W A, *Sens Actuat B-Chem*, 202 (2014) 144.
10 Kar P & Choudhury A, *Sens Actuat B-Chem,* 183 (2013) 25.
11 Ahuja T, Mir I A, Kumar D & Rajesh, *Biomaterials*, 28 (2007) 791.
12 Bhattacharya A, Ganguly K M, De A & Sarkar S, *Mater Res Bull,* 31 (1996) 527.
13 Galembeck A & Oswaldo L A, *Synth Met,* 84 (1997) 151.
14 Harreld J H, Dunn B & Nazar L F, *Int J Inorg Mater*, 1 (1999) 135.
15 Shi-Jain S & Kuramoto N, *Synth Met,* 114 (2000) 147.
16 Goyal S L, Sharma S, Jain D & Kishore N, *Indian J Pure Appl Phys,* 53 (2015) 456.
17 Chen W, Xingwei L, Gi X, Zhaoquang W & Wenquing Z, *Appl Surf Sci*, 218 (2003) 216.
18 De A, Ajay D & Susanta L, *Synth Met*, 144 (2004) 303.
19 Saeed M, Shakoor A & Ahmad E, *J Mater Sci*, 24 (2013) 3536.
20 Jundale D M, Navale S T, Khuspe G D, Dalavi D S, Patil P S & Patil V B, *J Mater Sci*, 24 (2013) 3526.
21 Asha, Goyal S L, Jain D & Kishore N, *J Chem Pharm Res,* 6 (2014) 105.
22 Manjunath S, Koppalkar R, Kumar A, Revanasiddappa M & Ambika P M V N, *Ferroelectric Lett*, 35 (2008) 36.
23 Machappa T & Ambika P M V N, *Physica B*, 404 (2009) 4168,
24 Koppalkar R, Kumar A, Parveen A, Badiger G R & Ambika P M V N, *Physica B,* 404 (2009) 1664.
25 Patil R, Roy A S, Koppalkar R, Kumar A, Jadhav K M & Ekhelikar S, *Composites: Part B,* 43 (2012) 3406.
26 Harun M H, Saion E, Kassim A, Hussain M Y, Mustafa I S & Omer M A A, *Malaysian Polym J*, 3 (2008) 24.
27 Ozkazanc E, Zor S & Ozkazanc H, *J Macromol Sci Phys*, 51 (2012) 2122.
28 Dey A, De S, De A & De S K, *Nanotechnology*, 15 (2004) 1277.
29 Pradhan D K, Choudhary R N P & Samantaray B K, *Mater Chem Phys*, 115 (2009) 557.
30 Gupta K, Chakraborty G, Jana P C & Meikap A K, *Solid State Commun*, 151 (2011) 573.
31 Asha, Goyal S L, Kumar D, Kumar S & Kishore N, *Indian J Pure Appl Phys*, 52 (2014) 341.
32 Sarkar A, Gosh P, Meikap A K, Chattopadhyay S K, Chatterjee S K, Chowdhury P, Roy K & Saha B, *J Appl Polym Sci,* 108 (2008) 2312.
33 De S, Dey A & De S K, *Eur Phys J B*, 46 (2005) 355.
34 Ozkazanc E, Ozkazanc H, Zor S & Abaci U, *Polym Eng Sci,* 51 (2011) 617.
35 De S, De A, Das A & De S K, *Mater Chem Phys*, 91 (2005) 477.
36 Papathanassiou A N, Sakellis I & Grammatikakis J, *Appl Phys Lett*, 91 (2007) 122911.
37 Elliott S R, *Adv Phys*, 36 (1987) 135.
38 Punia R, Kundu R S, Dult M, Murugavel S & Kishore N, *J Appl Phys*, 112 (2012) 083701.
39 Gosh M, Barman A, Meikap A K, De S K & Chatterjee S, *Phys Lett A*, 260 (1999) 138.
40 Mott N F, *Phil Mag,* 19 (1969) 835.
41 Patil S D, Raghavendra S C, Revansiddappa M, Narsimha P & Ambika P M V N, *Bull Mater Sci*, 30 (2007) 89.
42 Ozkazanc E, Zor S, Ozkazanc H, Guney H Y & Abaci U, *Mater Chem Phys*, 133 (2012) 356.
43 Bisquert J, Garcia-Belmonte G, Bueno P, Longo E & Bulhoes L O S, *J Electro Anal Chem,* 452 (1998) 229.
44 Sarkar A, Ghosh P, Meikap A K, Chattopadhyay S K, Chatterjee S K & Gosh M, *Solid State Commun*, 143 (2007) 358.
45 Yakuphanoglu F & Senkal B F, *Polym Adv Technol*, 19 (2008) 1876.
46 Soares B G, Leyva M E, Barra G M O & Khastgir D, *Eur Polym J*, 42 (2006) 676.
47 Lee H T, Leo C S & Chen S A, *Macromol Chem*, 194 (1993) 2433.
48 Ray D K, Himanshu A K & Sinha T P, *Indian J Pure Appl Phys*, 45 (2007) 692.
49 Tabellout M, Fatyeyeva K, Baillif P Y, Bardeau J F & Pud A A, *J Non Cryst Solids*, 351 (2005) 2835.
50 Kuleznev V N & Shershnev V A, *Chem Phys Polym*, (Mir Publishers, Moscow), 1990.